1 Micro-macro approach to cluster formation in granular media

S. Luding

Institute for Computer Applications 1, University of Stuttgart,
Pfaffenwaldring 27, 70569 Stuttgart, Germany
Particle Technology, DelftChemTech, TU Delft,
Julianalaan 136, 2628 BL Delft, The Netherlands
e-mail: lui@ica1.uni-stuttgart.de or s.luding@tnw.tudelft.nl
homepage: www.ica1.uni-stuttgart.de/~lui

Abstract

Dissipation in granular media leads to interesting phenomena as there are cluster formation and crystallization in non-equilibrium dynamical states. The freely cooling system is examined concerning the energy decay and the cluster evolution with time. Finally, an example is given for a possible micro-macro transition with respect to the flow variables density, velocity, and fluctuation kinetic energy.

Keywords:
inhomogeneous free cooling, clustering, cooperative phenomena, event-driven molecular dynamics, micro-macro transition

1.1 Introduction

Interesting phenomena can be observed when granular media are studied [6, 7, 18, 19]. The subject of this paper is the pattern formation via clustering in a dissipative, freely cooling system [2, 4, 14, 17]. The special behavior of granular media is connected to its ability to form a hybrid state between a fluid and a solid: Energy input leads to a reduction of the density due to more collisions, so that the material can flow, i.e. it becomes 'fluid'. On the other hand, in the absence of energy input, granular materials 'solidify' due to dissipation. This makes granular media an interesting multi-particle system with a rich phenomenology, however, theoretical approaches are non-classical and appear often extreemly difficult, so that there is still active research directed towards the understanding of granular media.

The basic ingredients of a granular model system are discussed briefly in section 1.2. The inhomogeneous cooling and clustering are described in detail in section 1.3. The basic idea is that in a freely cooling granular gas, fluctuations in density and temperature cause a position dependent energy loss.

Due to strong local dissipation, pressure and energy drop rapidly and material moves from 'hot' to 'cold' regions, leading to even stronger dissipation and thus causing the density instability with ever growing clusters.

In order to describe and understand such inhomogeneous, non-equilibrium systems, a particle simulation approach may be insufficient due to the enormous number of particles involved. However, a hydrodynamic theory of such dissipative granular flows is not available yet. Therefore, a first step towards a micro-macro transition that it neccessary to understand the hydrodynamic theory of granular media is presented. The density-, velocity-, and fluctuation kinetic energy-fields will be computed and discussed for the case of strong clustering.

1.2 Models for multi-particle simulations

The constituents of granular media are mesoscopic particles. When those objects interact (collide) the attractive potentials of the individual grains can be neglected. Two models for the repulsive particle-particle interactions are discussed in the following. They account for the excluded volume of the particles via a repulsive potential, either 'hard' or 'soft' and also account for dissipation in collisions via some coefficient of restitution. The third ingredient of a model granular material is friction which couples the rotational degrees of freedom to the linear motion, but it is not discussed in this paper.

The difference between the two most frequently used discrete element methods is the repulsive interaction potential. For the molecular dynamics (MD) method, soft particles with a power-law interaction potential are assumed, whereas for the event-driven (ED) method perfectly rigid particles are used. The consequence is that the duration of the contact of two particles, t_c, is finite for MD, but vanishes for ED.

1.2.1 The event-driven, rigid particle method

Consider two particles with diameter d_1 and d_2 and masses m_1 and m_2, The normal unit vector for their contact is $\boldsymbol{n}$, and $\boldsymbol{r}_i$ is the vector to the position of the center of particle i ($i = 1, 2$). The relative velocity of the contact points is $\boldsymbol{v}_c = \boldsymbol{v}_1 - \boldsymbol{v}_2$, with the velocity $\boldsymbol{v}_i$ of particle i. From momentum conservation it follows

$$\boldsymbol{v}_1' = \boldsymbol{v}_1 + \Delta\boldsymbol{P}/m_1 \quad \text{and} \quad \boldsymbol{v}_2' = \boldsymbol{v}_2 - \Delta\boldsymbol{P}/m_2 \ , \tag{1.1}$$

where $\boldsymbol{v}_i'$ is the unknown velocity of particle i after collision. The change of linear momentum of particle 1 is a function of the coefficient of restitution r:

$$\Delta\boldsymbol{P} = -m_{12}(1+r)\boldsymbol{v}_c^{(n)} \ , \tag{1.2}$$

with the reduced mass $m_{12} = m_1 m_2/(m_1 + m_2)$.

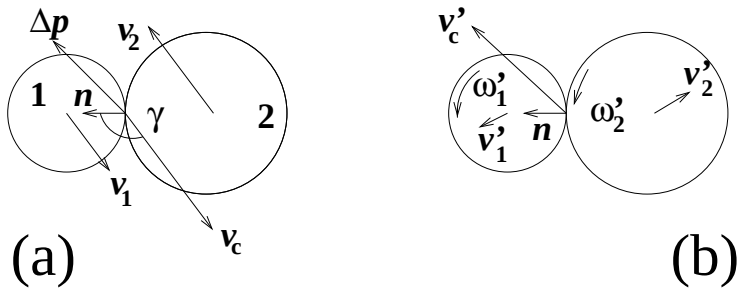

Fig. 1.1. Typical velocities of two particles immediately before (a) and just after (b) collision.

For the simulation of rigid particles, an event-driven method is used [9, 10, 14]. The particles undergo an undisturbed motion until an event occurs. An event can be either the collision of two particles or the collision of a particle with a wall. From the velocities just before contact, the particle velocities after a contact are computed following Eq. (1.1). Lubachevsky [9] introduced an efficient scalar ED algorithm which updates only those particles involved in the previous collision. The original algorithm is implemented and generalized to take into account dissipation.

1.2.2 The time driven, soft particle technique

Even without using the soft particle method [1, 3, 8] in this study, it is convenient to discuss briefly the standard approach. Replacing $\Delta \boldsymbol{P}$ in Eq. (1.1) by $\boldsymbol{f}(t)\Delta t_{\mathrm{MD}}$, with the molecular dynamics time step Δt_{MD}, allows the integration of the corresponding, discretized equations of motion with standard numerical methods [1].

Since the modeling of realistic deformations of the particles would be much too complicated, let us assume that the overlap of two particles is the only quantity important for the interaction potential. The interaction of two particles can be split into (at least) three independent forces, and is typically short range, i.e. the particles interact only when they are in contact. The first force, an elastic repulsive force proportional to the overlap, accounts for the excluded volume which each particle occupies. In the simplest case, a linear spring can be used. The second force, a viscous damping force, models the dissipation in the normal direction and is proportional to the relative velocity. The simplest possible dashpot is again linear. This linear spring-dashpot model can be solved analytically and leads to a constant contact duration t_c and a constant restitution coefficient r [11]. The third force, accounting for friction, acts in the tangential direction, but will not be discussed here; for more information see Refs. [6].

1.2.3 The connection between hard- and soft-sphere models

In the ED method, the time during which two particles are in contact is implicitly zero. The consequence is that exclusively pair contacts occur and the instantaneous momentum change $\Delta \boldsymbol{P}$ in Eq. (1.1) suffices to describe the collision. However, ED algorithms with constant r run into difficulties when the time between events, t_n, becomes too small – typically in systems with strong dissipation – and the so-called "inelastic collapse" occurs [16, 17], i.e. the collision rate diverges for a few particles in the system. Since this is an artefact of the hard sphere model, it is unphysical and has to be avoided. Because a diverging number of collisions is only possible if the contact duration vanishes, the physical contact duration t_c has to be reintroduced in order to allow for realistic ED simulations. In MD simulations, on the other hand, one has $t_c > 0$, since every contact takes some finite time. Therefore, only a limited amount of kinetic energy ($\Delta E \propto 1 - r^2$) can be dissipated per collision. A finite contact duration implies a finite energy dissipation rate. In contrast, the consequence of a diverging collision rate would be a diverging energy dissipation rate.

In a dense system of real particles, energy dissipation becomes ineffective, i.e. the 'detachment effect' occurs [12, 13]. This effect is not obtained with hard particles and a constant coefficient of restitution r. Therefore, in the framework of the so-called TC model, the restitution becomes elastic in nature, $r_n^{(i)} = 1$, if collisions occur too frequently, i.e. $t_n^{(i)} \leq t_c$, for the collision n of particle i. The time since the last collision is $t_n^{(i)}$ and the cut-off parameter t_c for elastic contacts can be identified with the contact duration. Thus, an additional material parameter is defined for the hard sphere model, that leads to qualitative agreement between ED and MD simulations and, in addition, avoids the inelastic collapse artefact. Recently, it has been shown that the TC model does not affect physical observables of the system, like the energy, as long as it is reasonably small [16].

1.3 Freely cooling granular media

The simulations presented in the following involve $N = 99856 = 316^2$ dissipative particles with the restitution coefficients $r = 0.9$, 0.8, and 0.6, in a periodic, quadratic system with volume fraction $\nu = 0.25$. The system size is $l = Ld$ with dimensionless size $L = 560$ and particle diameter $d = 1\,\mathrm{mm}$. In order to reach an equilibrated initial condition, the system is first allowed to equilibrate with $r = 1$ for several hundreds of collisions per particle, so that a Maxwellian velocity distribution and a homogeneous density can be found. Then, at $t = 0\,\mathrm{s}$, dissipation is activated and the quantities of interest are examined. Snapshots of the simulation with $r = 0.8$ are presented in Fig. 1.2 at different, rescaled times τ (see below).

The first picture in Fig. 1.2 is taken in the initally homogeneous cooling regime, whereas the next pictures show the different stages of the cluster

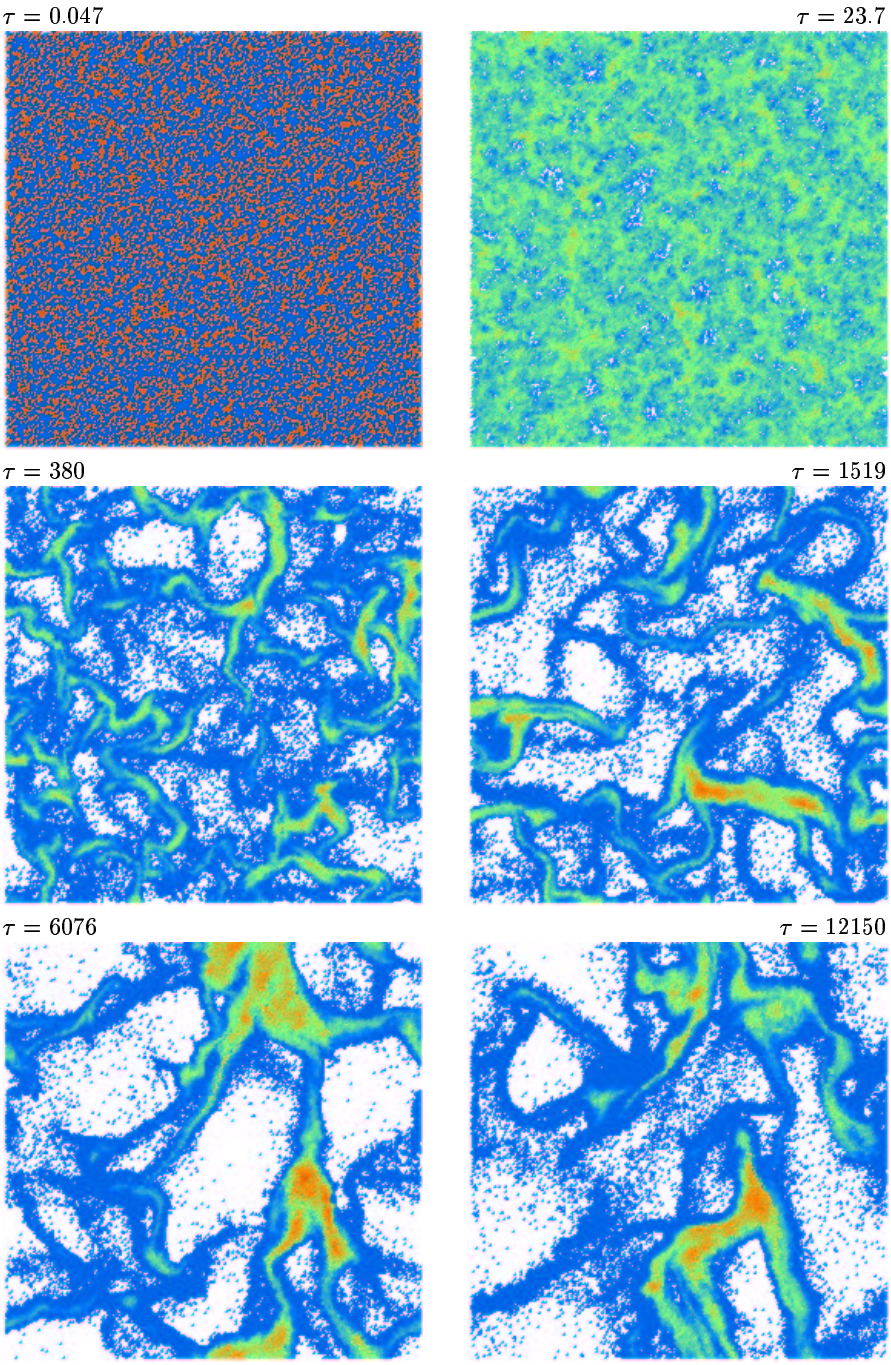

Fig. 1.2. ED simulation with $N = 99856$ particles in a system of size $L = 560$, volume fraction $\nu = 0.25$, restitution coefficient $r = 0.8$, and critical collision frequency $t_c^{-1} = 10^5\,\mathrm{s}^{-1}$. The collision frequency is color-coded: red, green and blue correspond to collision rates $t_n^{-1} \approx 50\,\mathrm{s}^{-1}$, $10\,\mathrm{s}^{-1}$ and $2\,\mathrm{s}^{-1}$, respectively.

growth regime. The final snapshots are taken in the limiting state, where the cluster has reached the system size. The particles are colored spots, where the green/red areas in the cluster centers correspond to particles with collision rate $t_n^{-1} \geq 50\,\mathrm{s}^{-1}$. This is much smaller than the critical collision rate $t_c^{-1} = 10^5\,\mathrm{s}^{-1}$, so that only a very small number of particles will be affected by the TC model.

1.3.1 Homogeneous and inhomogeneous cooling

In the homogeneous cooling state [5, 15, 17], one can expect that the kinetic energy $E = K(t)/K(0)$ of the system decays with time (the decay of energy with time is also evidenced by the change of color from red over orange to green and blue in Fig. 1.2) and follows the master-curve

$$E(\tau) = \frac{1}{(1+\tau)^2}\ , \tag{1.3}$$

with the dimensionless time $\tau = (1-r^2)t/(4t_E)$, the collision rate $t_E^{-1} = 8\nu g(\nu)\bar{v}/(\sqrt{\pi}d)$, the mean velocity $\bar{v} = \sqrt{K(t)/Nm}$, and the increased contact probability $g(\nu) = (1-7\nu/16)/(1-\nu)^2$ due to excluded volume effects at finite volume fractions ν. Inserting the parameters from the simulation, $1-r^2 = 0.36$, $g(\nu) \approx 1.5833$, and $\bar{v} = 0.02883\,\mathrm{m/s}$, one obtains an initial collision rate $t_E^{-1}(0) = 51.5\,\mathrm{s}^{-1}$ (corresponding to the red color in Fig. 1.2).

In Fig. 1.3, the normalized kinetic energy E and the normalized collision rate t_n^{-1}/t_E^{-1}, are presented, both as a function of the normalized time τ. At the beginning of the simulation we observe a perfect agreement between the theory for homogeneous cooling and the simulations. At $\tau \approx 10-40$ substantial deviations from the homogeneous cooling behavior become evident, i.e. the decay of energy is slowed down earlier for stronger dissipation. The deviation from the analytical form increases until $\tau \approx 10^3$ where the clusters reach system size and the behavior of E changes again to a slightly more rapid decrease.

This change in behavior is evident from the collision rate t_n^{-1}. At first, in the homogeneous cooling regime, the collision rate decays with $t_n^{-1} \propto \sqrt{E}$. Then the collision rate is almost constant (for $r = 0.9$ and $r = 0.8$) or even increases (for $r = 0.6$), until at $\tau \approx 10^3$ it becomes very noisy, indicating another change in the collective behavior. The long-time power law for the decay of energy with time is -2 in the homogeneous cooling case. In the cluster growth regime, however, we obtain slopes slightly smaller than -1 (the best fit leads to -0.920, -0.927, and -0.941 for $r = 0.9$, 0.8, and 0.6, respectively, with errors ± 0.002).

1.3.2 Cluster structure

In Fig. 1.4, the pair-correlation function during the clustering is plotted in order to visualize the short-range structure in the clusters. In Fig. 1.5, zooms

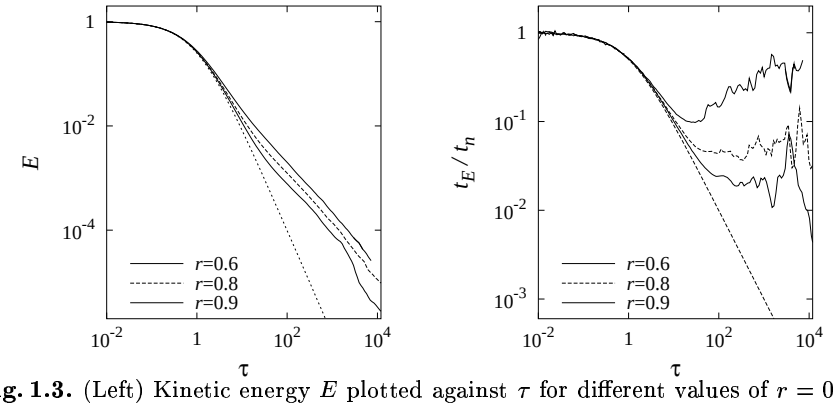

Fig. 1.3. (Left) Kinetic energy E plotted against τ for different values of $r = 0.9$, 0.8, and 0.6. The dotted line represents Eq. (1.3). (Right) Normalized collision rate t_E/t_n plotted against τ. The dashed line represents the collision rate $\sqrt{E}$ in the homogenously cooling case.

into the bottom-right area of the system in Fig. 1.2 are presented in order to give a more direct picture. In the initial state, the system is rather disordered and homogeneous. In the cluster growth regime, some particles approach closer and form loose clusters, however, the structure is still disordered, fluid-like. Only in the very late stage of the simulation, where the clusters are very large, one obtains crystalline, triangular lattice structures with a peculiar distribution of collision rates as color-coded.

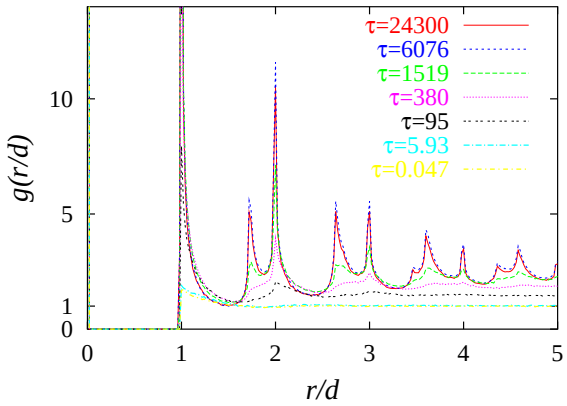

Fig. 1.4. Correlation function $g(r/d)$ as obtained from the simulation in Fig. 1.2 with τ as given in the inset.

This more qualitative picture can also be verified by computing the particle correlation function $g(r/d)$, see Fig. 1.4. The data are displayed for dif-

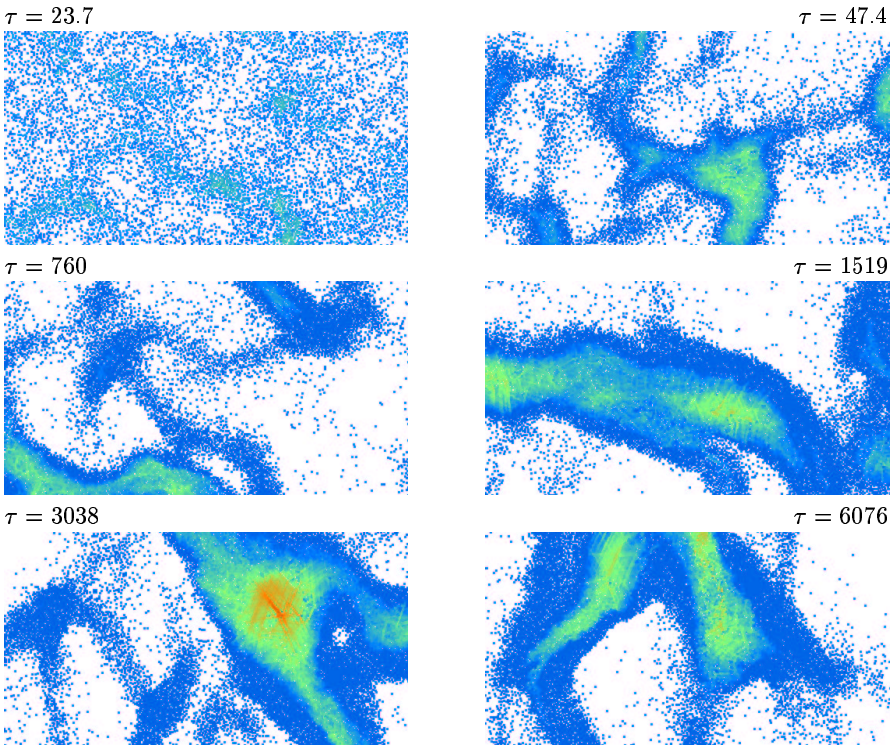

Fig. 1.5. Zooms into the lower right part of the ED simulation from Fig. 1.2.

ferent τ-values, showing that the structure in the system becomes more and more pronounced with increasing time. Like the zoom-in in Fig. 1.5, also the correlation function shows that the crystalline structure occurs only in the late regime where the clusters are very large, with 'frozen' cores. Pronounced peaks at 1, $\sqrt{3}$, 2, ... indicate a triangular order of the particles.

1.3.3 Cluster growth

The cluster growth can be studied quantitatively in the spirit of Luding and Herrmann [14]. All particle pairs with a distance smaller than some cut-off distance $\delta < (1 + S)d$, with an arbitrary cut-off parameter $S = 0.1$, are assumed to belong to the same cluster. After all particle pairs are examined, one obtains a cluster-size distribution and its moments. The first moment, the mean cluster size $\langle M \rangle$, and the size of the largest cluster M_{max} are plotted in Fig. 1.6 against the time τ.

Both values are almost constant in the initial, homogeneous cooling regime. In the cluster growth regime a rapid increase of both $\langle M \rangle$ and M_{max} is evidenced until, at larger τ, the values reach a maximum and seemingly saturate or even decrease in the final regime where the clusters have reached system

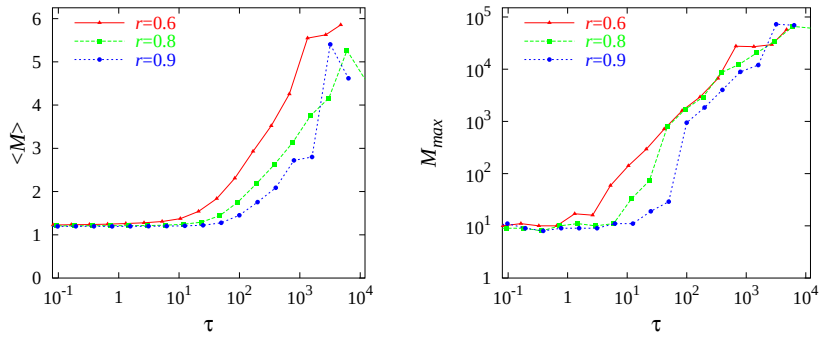

Fig. 1.6. (Left) Mean cluster size and (Right) Maximum cluster size as funtions of time τ for different coefficients of restitution r.

size. The cluster growth startes earlier for stronger dissipation, but the largest cluster seems to grow more rapidly for weaker dissipation, however, at a later time.

1.3.4 Micro-macro transition

In this subsection, the macroscopic field quantities density, velocity, and fluctuation kinetic energy are discussed. In order to obtain the fields from the simulation data, the system is arranged on a 50×50 grid and the field quantities are computed for every cell. The density $\nu(x, y) = n_c \pi a^2 / V_c$ and the fluctuation kinetic energy $e(x, y) = (m/2) \sum_{i \in c} [\boldsymbol{v}_i - \boldsymbol{v}(x, y)]^2 / n_c$, are plotted in Fig. 1.7. The symbols are the number of particles per cell n_c, the cell-volume V_c, the particle radius a, mass m, and the mean velocity $\boldsymbol{v}(x, y) = \sum_{i \in c} \boldsymbol{v}_i / n_c$ in the cell.
The iso-lines of the density are chosen such that the dilute area ($\nu < 0.1$ – pink) is visible as well as the coexistence area between fluid and solid regions ($0.6 < \nu < 0.8$ – between blue and green). The green islands are solid clusters with triangular arrangement, whereas the pink islands are almost empty regions. Between pink and blue, the fluid phase exists at almost all densities.

The iso-lines for the fluctuation kinetic energy are chosen in arbitrary units. However, it is evident, that the temperature and the density fields are not correlated in a simple fashion. Dense regions are not neccessarily cold neither are dilute regions neccessarily hot. The structure of the e-field appears more detailed than the structure of the density field.

Finally, the velocity vector field is plotted as momentum flux field in Fig. 1.8 and shows the mass-flux in the system. A closer examination leads to the conclusion that the clusters are not stable, but have remaining internal motion due to shear- or compressive modes. Note that also the velocity field

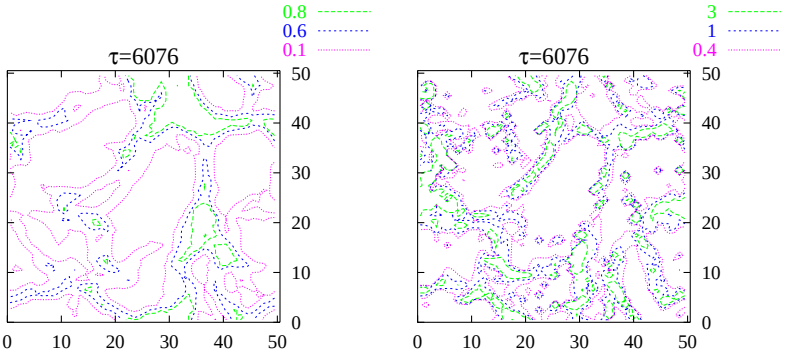

Fig. 1.7. Density and fluctuation kinetic energy iso-lines for the snapshot at time $\tau = 6076$ in Fig. 1.2. The density is given as volume fraction, whereas the energy is given in arbitrary units.

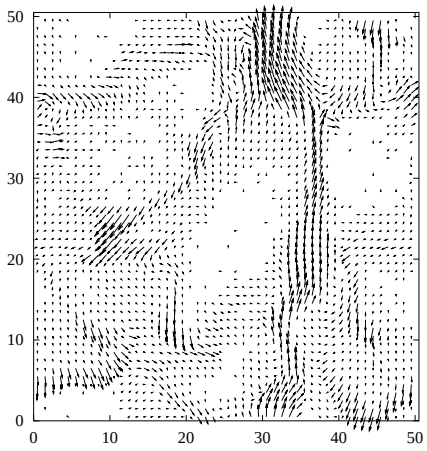

Fig. 1.8. Momentum flux field $\nu \boldsymbol{v}$ for the snapshot with $\tau = 6076$ in Fig. 1.2.

(energy due to flux motion) is not directly correlated to the fluctuation kinetic energy.

1.4 Summary and Conclusion

With a rather simple description of a granular material as an ensemble of inelastic hard disks (spheres), we have investigated the interesting effect of clustering in freely cooling systems. For short times the system is disordered and gas-like, whereas the structures at larger times are dense, crystalline clusters. The clusters grow until they reach the system size. Simulations at

very long times were possible with the TC model, which reduces dissipation when contacts become too frequent.

As a first step towards a macroscopic, hydrodynamic description of clustering in freely cooling granular media, the density, the velocity and the fluctuation kinetic energy were computed from the simulation snapshots. The density field is directly correlated with the snapshot, whereas neither velocity nor fluctuation kinetic energy are directly correlated with the density. The latter fact implies that all three quantities are independent variables, neccessary for a hydrodynamic description of the system.

Further investigations concerning the transport parameters pressure, viscosity and heat conductivity in similar systems are in progress in two dimensional model systems and are to be applied to a successful hydrodynamic theory of granular flow.

Achnowledgements

We acknowledge the financial support of the Deutsche Forschungsgemeinschaft (DFG) and of the Max-Planck PKS in Dresden.

References

1. M. P. Allen and D. J. Tildesley. *Computer Simulation of Liquids.* Oxford University Press, Oxford, 1987.
2. R. Cafiero, S. Luding, and H. J. Herrmann. Two-dimensional granular gas of inelastic spheres with multiplicative driving. *Phys. Rev. Lett.*, 84:6014–6017, 2000.
3. P. A. Cundall and O. D. L. Strack. A discrete numerical model for granular assemblies. *Géotechnique*, 29(1):47–65, 1979.
4. I. Goldhirsch and G. Zanetti. Clustering instability in dissipative gases. *Phys. Rev. Lett.*, 70(11):1619–1622, 1993.
5. P. K. Haff. Grain flow as a fluid-mechanical phenomenon. *J. Fluid Mech.*, 134:401–430, 1983.
6. H. J. Herrmann, J.-P. Hovi, and S. Luding, editors. *Physics of dry granular media - NATO ASI Series E 350*, Dordrecht, 1998. Kluwer Academic Publishers.
7. Y. Kishino, editor. *Powders & Grains 2001*, Rotterdam, 2001. Balkema.
8. M. Lätzel, S. Luding, and H. J. Herrmann. Macroscopic material properties from quasi-static, microscopic simulations of a two-dimensional shear-cell. *Granular Matter*, 2(3):123–135, 2000. cond-mat/0003180.
9. B. D. Lubachevsky. How to simulate billards and similar systems. *J. of Comp. Phys.*, 94(2):255, 1991.
10. S. Luding. Granular materials under vibration: Simulations of rotating spheres. *Phys. Rev. E*, 52(4):4442, 1995.
11. S. Luding. Collisions & contacts between two particles. In H. J. Herrmann, J.-P. Hovi, and S. Luding, editors, *Physics of dry granular media - NATO ASI Series E350*, page 285, Dordrecht, 1998. Kluwer Academic Publishers.

12. S. Luding, E. Clément, A. Blumen, J. Rajchenbach, and J. Duran. Anomalous energy dissipation in molecular dynamics simulations of grains: The "detachment effect". *Phys. Rev. E*, 50:4113, 1994.
13. S. Luding, E. Clément, A. Blumen, J. Rajchenbach, and J. Duran. Interaction laws and the detachment effect in granular media. In *Fractal Aspects of Materials*, volume 367, pages 495–500, Pittsburgh, Pennsylvania, 1995. Materials Research Society, Symposium Proceedings.
14. S. Luding and H. J. Herrmann. Cluster growth in freely cooling granular media. *Chaos*, 9(3):673–681, 1999.
15. S. Luding, M. Huthmann, S. McNamara, and A. Zippelius. Homogeneous cooling of rough dissipative particles: Theory and simulations. *Phys. Rev. E*, 58:3416–3425, 1998.
16. S. Luding and S. McNamara. How to handle the inelastic collapse of a dissipative hard-sphere gas with the TC model. *Granular Matter*, 1(3):113–128, 1998. cond-mat/9810009.
17. S. McNamara and W. R. Young. Dynamics of a freely evolving, two-dimensional granular medium. *Phys. Rev. E*, 53(5):5089–5100, 1996.
18. T. Pöschel and S. Luding, editors. *Granular Gases*, Berlin, 2001. Springer. Lecture Notes in Physics 564.
19. P. A. Vermeer, S. Diebels, W. Ehlers, H. J. Herrmann, S. Luding, and E. Ramm, editors. *Continuous and Discontinuous Modelling of Cohesive Frictional Materials*, Berlin, 2001. Springer. Lecture Notes in Physics 568.